energies

MDPI

Article

Two-Stage Optimal Scheduling Based on the Meteorological Prediction of a Wind–Solar-Energy Storage System with Demand Response

Lu Wei [1,*], Yiyin Li [1], Boyu Xie [1], Ke Xu [2] and Gaojun Meng [2]

[1] Henan Meteorological Service Center, Zhengzhou 450003, China
[2] School of Electric Power Engineering, Nanjing Institute of Technology, Nanjing 211167, China; xukesam@njit.edu.cn (K.X.); gjun_m@njit.edu.cn (G.M.)
* Correspondence: j0000003013@njit.edu.cn

Abstract: With large-scale wind and solar power connected to the power grid, the randomness and volatility of its output have an increasingly serious adverse impact on power grid dispatching. Aiming at the system peak shaving problem caused by regional large-scale wind power photovoltaic grid connection, a new two-stage optimal scheduling model of wind solar energy storage system considering demand response is proposed. There is a need to comprehensively consider the power generation cost of various types of power sources, day-ahead load forecasting information, and other factors and plan the day-ahead output plan of the energy storage system with the minimum system operation cost as the optimization objective of day-ahead dispatching. The demand response strategy is introduced into the time-ahead optimal scheduling, and the optimization of the output value of the energy storage system in each period is studied with the goal of minimizing the system adjustment cost. The particle swarm optimization algorithm is used to solve the model, and the IEEE33 node system is used for an example simulation. The results show that using the demand response and the collaborative effect of the energy storage system can suppress the uncertainty of wind power and photovoltaic power, improve the utilization rate of the system, reduce the power generation cost of the system, and achieve significant comprehensive benefits.

Keywords: demand response; energy storage system; two-stage scheduling; particle swarm optimization algorithm

Citation: Wei, L.; Li, Y.; Xie, B.; Xu, K.; Meng, G. Two-Stage Optimal Scheduling Based on the Meteorological Prediction of a Wind–Solar-Energy Storage System with Demand Response. *Energies* **2024**, *17*, 1286. https://doi.org/10.3390/en17061286

Academic Editors: Adrian Ilinca and Abdul-Ghani Olabi

Received: 9 January 2024
Revised: 9 February 2024
Accepted: 25 February 2024
Published: 7 March 2024

1. Introduction

With the large-scale integration of new energy into the grid, the instability and anti-peak regulation of its power generation output greatly increases the adjustment burden of the system [1]. This indirectly implies that vigorously improving the flexible regulation capacity of the power system, ensuring the balance of power supply and demand at different time scales, as well as the high-level absorption of new energy, is not only inherently demanded to speed up the construction of a new power system with new energy as the main body, but it is also an urgent requirement for the promotion of the realization of a carbon peak in 2030 and carbon neutralization in 2060 [2–4].

With the increase in the proportion of new energy access, the research on responding to the volatility and randomness of new energy by demand response has increased sharply [5,6]. In reference [7], a demand response scheduling strategy with multi-time scale rolling coordination was designed, which calls for a flexible load to track wind power rolling. In reference [8], a multi-objective optimization model of source–load coordination was established to maximize the absorption of wind power and minimize the operating cost of the system. In reference [9], a power system stochastic dispatching model considering large-scale wind power and demand response was established. In reference [10], a day-ahead optimization model of the power system was constructed by introducing

time-sharing electricity price and interruptible load into a large-scale wind power system. In addition, the effects of two kinds of demand response resources to reduce the reverse peak regulation performance of wind power and the impact of intermittence on the power system were compared.

At present, there is almost no research on the analysis and modeling of demand response uncertainty [11]. Reference [12] analyzed the causes of the uncertainty of demand response resources and attributed the causes of the uncertainty to the uncertainty of the model and forecast. Reference [13] established the random response model of price type load. The uncertainty of price type load response is regarded as a random injection variable and introduced into the random interactive probabilistic power flow model of source load. Reference [14] artificially sets the range of uncertain demand response and reserves the uncertain response within this range so that the economy of the system is the highest. Reference [15] studied the incentive demand response and price demand response, and the scheduling cost models under uncertain response were established, respectively. The above literature provides a good theoretical basis for the uncertainty analysis of demand response. However, these studies focus on the modeling of the influencing factors of demand response uncertainty and analyze the relationship between influencing factors and demand response uncertainty, which cannot provide a more practical reference for power system dispatching.

In summary, this work constructs a two-stage optimal scheduling model of land-scape storage considering demand response, analyzes the load characteristics of the user side, and designs a DR model that integrates direct load control (DLC) and transferable load (TL) to make the load and new energy generation closer in timing. Subsequently, the scheduling optimization model of the day-ahead and the first two stages of the landscape storage system is established, and the demand response strategy is introduced in the pre-time scheduling phase to realize the comprehensive optimization of load demand distribution and energy storage output planning. Finally, the IEEE33 node system is taken as the simulation system to analyze the effect of the proposed model on the landscape ab-sorption ability of the system.

2. Load Characteristic Analysis and DR Modeling

2.1. User Side Load Characteristic Analysis

According to the way that the power system participates in the demand response, the customer-side load is divided into four categories [16]: (1) basic load: it belongs to uncontrollable load, which is fully responsive to the needs of users, and the system cannot change its energy use mode and time; (2) translational load: the power supply time of the load can be changed according to the plan, the load needs to be shifted as a whole, and the power absorption time spans multiple scheduling periods; (3) a load that can be reduced: it can withstand a certain interruption or power reduction, reduce the load running for a certain time, and reduce some or all of it according to supply and demand; and (4) transferable load: the electricity absorption in each time period can be adjusted flexibly, but the total load in the whole cycle should remain unchanged after transfer and before transfer.

2.2. Demand Response Modeling

2.2.1. DLC Model of Daily Electricity Absorption

The load of DLC is directly reduced by the load control device of the power company during the peak load, which is mainly aimed at residential or small commercial users and other domestic electricity users. The response characteristic of the participating load is that the load can be reduced, which belongs to peak-cutting resources, such as air conditioners, electric water heaters, and other loads with cold and hot storage capacity [17]. According

to the dispatching needs and load distribution, multiple groups of users are involved in the DLC project, and the load reduction $F_{DLC}(t)$ in the period t is as follows:

$$F_{DLC}(t) = \sum_{i=1}^{I} \alpha_i(t) F_{DLC,i}(t) \tag{1}$$

where $F_{DLC,i}(t)$ represents the reducible load of i-th group user in the time t, $\alpha_i(t)$ represents 0–1 variable, $\alpha_i(t) = 1$ indicates that the load of i-th group is reduced, and $\alpha_i(t) = 0$ indicates that the load of i-th group is not reduced.

In order to encourage users to implement DLC, power suppliers will give electricity price compensation to participating users, and the rate of electricity price compensation that users can obtain when they participate in DLC is proportional to the degree of load reduction. Let the basic compensation rate of the DLC project be $\lambda_{0,DLC}(\lambda_{0,DLC} \in (0,1))$, then the actual electricity price compensation rate $\lambda_i(t)$ of i-th group users in the time t is

$$\lambda_i(t) = \lambda_{0,DLC}(t)\left[\frac{\alpha_i(t) F_{DLC,i}(t)}{1.2 F_i(t)}\right] \tag{2}$$

where $F_i(t)$ represents the planned participation load of i-th group users in time t.

The load reduction compensation provided by the power supplier, that is, the DLC cost, is

$$C_{DLC} = \sum_{i=1}^{I} \sum_{t=1}^{T} \lambda_i(t) P_1(t) \alpha_i(t) F_{DLC,i}(t) \Delta t \tag{3}$$

where $P_1(t)$ represents the domestic electricity price of the time t, T represents the number of scheduling periods, and Δt represents the scheduling step, with a value of 1 h.

2.2.2. TL Model of Industrial Power Absorption

TL entails users controlling themselves after receiving the system instruction signal; turn out or transfer to the load, mainly for large industrial users and other industrial power users; and that the response characteristic of the participating load is movable load. It is a kind of peak-cutting and valley-filling resource, and it is generally the industrial assembly line load that can be arranged for downtime production. There are K groups of users to participate in the TL project, and the transfer load $F_{TL}(t)$ in the time t is

$$F_{TL}(t) = \sum_{k=1}^{K} \rho(t) \alpha_k(t) F_{TL,k}(t) \tag{4}$$

where $F_{TL,k}(t)$ represents the transferable load of k-th group users in the time t, turning in is negative, turning out is positive; $\alpha_k(t)$ is 0–1 variable, $\alpha_k(t) = 1$ indicates that the load is selected, $\alpha_k(t) = 0$ indicates that the load is not selected, $\rho(t)$ represents the probability that the user obeys the power grid regulation and control, taking into account the uncertainty of user obedience, increases the load margin, which is more conducive to the stability of the system.

Similarly, the participating users of the DLC project are compensated according to the TL project, and the actual electricity price compensation rate $\lambda_k(t)$ and the TL cost C_{TL} are

$$\lambda_k(t) = \lambda_{0,TL}(t)\left[\frac{\left|\rho(t) \alpha_k(t) F_{TL,k}(t)\right|}{1.2 F_k(t)}\right] \tag{5}$$

$$C_{TL} = \sum_{k=1}^{K} \sum_{t=1}^{T} \lambda_k(t) P_2(t) \left|\rho(t) \alpha_k(t) F_{TL,k}(t)\right| \Delta t \tag{6}$$

where $\lambda_{0,TL}$ represents the basic compensation rate of TL, $F_{k(t)}$ represents the planned participation load of k-th group users in time t, and $P_2(t)$ represents industrial electricity price in time t.

2.2.3. DR Comprehensive Model

In order to reduce the load more quickly and reliably during the peak hours of power absorption and to better improve the timing matching between load and new energy generation, the proposed DR comprehensive model takes into account both DLC and TL models. Then, the load $F_{DR}(t)$ and the total call cost C_{DR} of DR after the implementation of DR in time t is

$$F_{DR}(t) = F_{initial}(t) - F_{DLC}(t) - F_{TL}(t) \tag{7}$$

$$C_{DR} = C_{DLC} + C_{TL} \tag{8}$$

where $F_{initial}(t)$ represents the initial load of time t.

2.3. User Satisfaction Degree

Users are important participants in the electricity market, and the implementation of DR will have an impact on their power comfort. Considering the scale of user participation, user satisfaction should be taken into account when implementing DR [18]. Customer satisfaction requires that the electricity demand is met in time, and the lower the load reduction or transfer, the higher the satisfaction.

$$\begin{cases} M_{DLC} = \frac{1}{I}\sum_{i=1}^{I}\sum_{t=1}^{T}[1 - \frac{\alpha_i(t)F_{DLC,i}(t)}{F_i(t)}] \\ M_{TL} = \frac{1}{K}\sum_{k=1}^{K}\sum_{t=1}^{T}[1 - \frac{|\rho(t)\alpha_k(t)F_{TL,k}(t)|}{F_k(t)}] \\ M_{user} = \frac{1}{2}(M_{DLC} + M_{TL}) \end{cases} \tag{9}$$

where M_{DLC} and M_{TL} are the average user satisfaction of DLC and TL, respectively, and M_{user} is the comprehensive satisfaction of users.

3. Two-Stage Optimal Scheduling Model of Scenery Storage

3.1. Day-Ahead Scheduling Model

With the goal of minimizing the operating cost of the system, the output arrangement of the day-ahead energy storage system is established, and the objective function is as follows:

$$\min C_1 = C_H + C_W + C_{PV} + C_{ESS} \tag{10}$$

where C_1 represents the total operation cost of the whole dispatching cycle of the system, C_H represents the operation cost of the thermal power plant, C_W represents the cost of wind power generation, C_{PV} represents the cost of photovoltaic power generation, and C_{ESS} represents the operation cost of energy storage.

$$C_H = \sum_{t=1}^{T_1}\sum_{i=1}^{n_H} c_{H,i}p_{H,i}(t) \tag{11}$$

where T_1 represents the number of periods in a day-ahead dispatching cycle, n_H represents the number of thermal power units, $c_{H,i}$ represents the coal-fired cost of thermal power unit i, $p_{H,i}(t)$ represents the active power output of thermal power unit i at time t.

$$C_W = \sum_{t=1}^{T_1}\sum_{i=1}^{n_W} c_{W,i}p_{W,i}(t) \tag{12}$$

where n_W represents the number of wind farms, $c_{W,i}$ represents the power generation cost of wind farm i, $p_{W,i}(t)$ represents the active power output of wind farm i at time i.

$$C_{PV} = \sum_{t=1}^{T_1}\sum_{i=1}^{n_{PV}} c_{PV,i}p_{PV,i}(t) \tag{13}$$

where n_{PV} represents the number of photovoltaic power stations, $c_{PV,i}$ represents the power generation cost of photovoltaic power station i, $p_{PV,i}(t)$represents the active power output of photovoltaic power station i at time t.

$$C_{ESS} = \sum_{t=1}^{T_1} \sum_{i=1}^{n_{ESS}} c_{ESS,i}[e_{ch,i}(t)p_{ESS,i}(t)(1-\eta_{ch,i}) + e_{dis,i}(t)p_{ESS,i}(t)(1-\eta_{dis,i})] \quad (14)$$

where n_{ESS} represents the number of energy storage power stations, $c_{ESS,i}$ represents the operating cost of energy storage power station i, $p_{ESS,i}(t)$ represents the active power output of energy storage power station i at time t, $e_{ch,i}(t)$ and $e_{dis,i}(t)$ represent the state variables of energy storage charge and discharge of energy storage power station i at time t, with values of 0 or 1. When the energy storage is charged, $e_{ch,i}(t) = 1$; when the energy storage is discharged, $e_{dis,i}(t) = 1$, and $e_{ch,i}(t)e_{dis,i}(t) = 0$; $\eta_{ch,i}$ and $\eta_{dis,i}$ are the charging efficiency and discharging efficiency of the energy storage power station i, respectively.

The constraints of the day-ahead scheduling model are as follows:

(1) Power balance constraints:

$$p_{load}(t) = \sum_{i=1}^{n_H} p_{H,i}(t) + \sum_{i=1}^{n_W} p_{W,i}(t) + \sum_{i=1}^{n_{PV}} p_{PV,i}(t) + \sum_{i=1}^{n_{ESS}} p_{ESS,i}(t) \quad (15)$$

where $p_{load}(t)$ represents the total load at time t.

(2) Upper and lower limits of power generation output:

$$\begin{cases} p_{H,i}^{min} \le p_{H,i}(t) \le p_{H,i}^{max} \\ 0 \le p_{W,i}(t) \le p_{W,i}^{max} \\ 0 \le p_{PV,i}(t) \le p_{PV,i}^{max} \end{cases} \quad (16)$$

where $p_{H,i}^{min}$ and $p_{H,i}^{max}$ represent the minimum and maximum technical output of thermal power unit i; $p_{W,i}^{max}$ and $p_{PV,i}^{max}$ represent the maximum theoretical output of wind farm i and photovoltaic power station i, respectively.

(3) Climbing rate constraint:

$$\begin{cases} R_{H,i}^{d} \le p_{H,i}(t) - p_{H,i}(t-1) \le R_{H,i}^{u} \\ R_{W,i}^{d} \le p_{W,i}(t) - p_{W,i}(t-1) \le R_{W,i}^{u} \\ R_{PV,i}^{d} \le p_{PV,i}(t) - p_{PV,i}(t-1) \le R_{PV,i}^{u} \end{cases} \quad (17)$$

where $R_{H,i}^{d}$ and $R_{H,i}^{u}$ represent the lower limit and upper limit of the ramp rate of thermal power unit i, respectively; $R_{W,i}^{d}$ and $R_{W,i}^{u}$ represent the lower limit and upper limit of the ramp rate of wind farm i, respectively; $R_{PV,i}^{d}$ and $R_{PV,i}^{u}$ represent the lower limit and upper limit of the ramp rate of photovoltaic power station i, respectively.

(4) Energy storage active output constraints:

$$p_{ESS,i}^{min} \le p_{ESS,i}(t) \le p_{ESS,i}^{max} \quad (18)$$

where $p_{ESS,i}^{min}$ and $p_{ESS,i}^{max}$ represent the lower limit value and upper limit value of the active power output of the energy storage power station i, respectively.

(5) Energy storage SOC constraints:

$$soc_{min,i} \le soc_i(t) \le soc_{max,i} \quad (19)$$

where $soc_i(t)$ represents the state of charge of energy storage power station i at time t; $soc_{min,i}$ and $soc_{max,i}$ represent the lower and upper limit of the state of charge of energy storage power station i, respectively.

In order to prevent the battery from being overcharged and overdischarged for a long time and prolong the energy storage life, this paper determines the priority and size of the output of each energy storage power station according to the SOC real-time status of the energy storage battery and reasonably arranges the current output plan of the energy storage system. The charge and discharge margin coefficients $C\%$ and $D\%$ are introduced to measure the dispatchability of each energy storage power station. The higher the value of $C\%$ and $D\%$, the greater the dispatchability and the priority output of the energy storage power station. The calculation equation is as follows:

$$C\% = \frac{soc_{\max,i} - soc_i(t)}{soc_{\max,i}} \times 100\% \tag{20}$$

$$D\% = \frac{soc_i(t) - soc_{\min,i}}{soc_{\min,i}} \times 100\% \tag{21}$$

3.2. Pre-Time Scheduling Model

The pre-time optimal scheduling model is based on the planned output curve of the day-ahead energy storage system and aims to minimize the system adjustment cost according to the user-side demand response. The adjustment cost mainly includes the adjustment cost of load participation demand response and the adjustment cost of modified energy storage output. The objective function is as follows:

$$\min C_2 = \sum_{t=1}^{T_2} [C_{\mathrm{DR}}(t) + \sum_{i=1}^{n_{\mathrm{ESS}}} w_{\mathrm{ESS},i}(t) \left| p_{\mathrm{ESS},i}(t) - p'_{\mathrm{ESS},i}(t) \right|] \tag{22}$$

where T_2 represents the number of periods in the pre-scheduling cycle, C_2 represents the adjustment cost of the whole scheduling cycle of the system, $C_{\mathrm{DR}}(t)$ represents the total DR call cost at time t, $w_{\mathrm{ESS},i}(t)$ represents the adjustment cost coefficient of the energy storage power station i, $p_{\mathrm{ESS},i}(t)$ represents the active power output of the energy storage power station i in the pre-time dispatching, $p'_{\mathrm{ESS},i}(t)$ represents the day-ahead dispatching plan value of the energy storage power station i active power output.

The constraints of the pre-time scheduling model are as follows:

(1)~(5) is similar to the equation in the day-ahead scheduling constraint.

(6) DR model-related constraints:

$$\alpha_i(t) F_{\mathrm{DLC},i}(t) \le F_i(t) \tag{23}$$

$$\left| \rho(t) \alpha_k(t) F_{\mathrm{TL},k}(t) \right| \le F_k(t) \tag{24}$$

(7) User satisfaction constraint:

$$M_{\mathrm{user}} \ge M_{\mathrm{user}}^{\min} \tag{25}$$

where $M_{\mathrm{user}}^{\min}$ represents the set minimum user satisfaction.

4. Evaluation Index

4.1. Peak-to-Valley Ratio

The greater the load peak-to-valley ratio, the more frequent the start-up and shutdown of the thermal power unit or the operation in the state of deep peak regulation, which affects the economic operation of the unit and interferes with the safety and stability of the system. Both DR and ESS can cut the peak, fill the valley, and reduce the ratio of peak to valley. The peak/valley ratio μ is defined as the ratio of the maximum load to the minimum

load in a statistical period t. The smaller the value of μ, the better the effect of peak-cutting and valley-filling:

$$\mu = \frac{\max[F_{DR}(t) - p_{ESS}(t)]}{\min[F_{DR}(t) - p_{ESS}(t)]} \tag{26}$$

4.2. New Energy Absorption Rate

If the problem of trans-regional energy transmission is not considered, the new energy absorption is mainly related to the regulation performance of thermal power units (maximum and minimum technical output, power installation growth rate), load scale and peak–valley difference, energy storage scale, and maximum charging rate. The new energy absorption rate is defined as the ratio of the actual output of the new energy to its theoretical output [19]. The calculation equation is as follows:

$$\begin{cases} R_W = \frac{Q_{W,act}+Q_{W,ESS}}{Q_{W,th}} \\ R_{PV} = \frac{Q_{PV,act}+Q_{PV,ESS}}{Q_{PV,th}} \\ R_{new} = \frac{Q_{new,act}+Q_{new,ESS}}{Q_{new,th}} \end{cases} \tag{27}$$

where R_W, R_{PV}, and R_{new} represent wind, photovoltaic, and total new energy absorption rate, respectively; $Q_{W,act}$, $Q_{PV,act}$, and $Q_{new,act}$ represent the direct output of wind, photovoltaic, and total new energy, respectively; $Q_{W,th}$, $Q_{PV,th}$, and $Q_{new,th}$ represent the theoretical output of wind, photovoltaic, and total new energy, respectively; $Q_{W,ESS}$, $Q_{PV,ESS}$, and $Q_{new,ESS}$ represent wind power, photovoltaic, and total new energy stored by ESS, respectively.

5. Case Analysis

5.1. Simulation Scenario Setting

Four kinds of system simulation scenarios are set to analyze the influence of the energy storage system and demand response on the peak-cutting, valley-filling, and landscape-absorbing ability of the system.

Case 1: The base scenario, which does not introduce energy storage systems and demand responses.

Case 2: The energy storage scenario, in which only the energy storage system is introduced, and four groups of energy storage are set up, each with a capacity of 50 MW·h. Other parameters are shown in the following section.

Case 3: The demand response scenario, which only introduces demand response. The proportion of planned participation load of DLC and TL projects to the total load is set to 0.05 and 0.08, respectively.

Case 4: The comprehensive scenario in which both demand response and energy storage systems are introduced. The specific parameters are the same as in Case 2.

5.2. Basic Data

This work is analyzed by taking the improved IEEE33 system as an example. The basic data of 10 thermal power units, DR and ESS, are shown in Tables 1–3, respectively. V_0 is the initial capacity of ESS.

The installed capacity of wind farms and photovoltaic power stations is 1500 and 500 MW, respectively. As shown in Figure 1, the photovoltaic output curve is set according to the photovoltaic power generation forecasting model, and the wind power output and load curve are set according to the historical forecast data. Assuming that the wind farm and photovoltaic power station are arranged to generate electricity according to the forecast, the costs of wind power and photovoltaic are 0.42 and 0.63 CNY $(kW{\cdot}h)^{-1}$, respectively. In order to facilitate statistics, it is assumed that the user load changes of each group of DR projects are equal in one day, and the proportion of planned participation load to the total load of DLC and TL projects is 0.05 and 0.08, respectively.

Table 1. The basic data of thermal power unit.

Thermal Power	$p_{H,i}^{min}$/MW	$p_{H,i}^{max}$/MW	$R_{H,i}^{d}$/(MW·h^{-1})	$R_{H,i}^{u}$/(MW·h^{-1})	$c_{H,i}$/[yuan·(kW·h)$^{-1}$]
No. 1	150	400	−160	160	0.23
No. 2	120	300	−100	100	0.25
No. 3	120	300	−100	100	0.25
No. 4	100	300	−80	80	0.26
No. 5	100	300	−80	80	0.26
No. 6	100	300	−80	80	0.26
No. 7	50	200	−50	50	0.31
No. 8	50	200	−50	50	0.31
No. 9	50	200	−50	50	0.31
No. 10	50	200	−50	50	0.31

Table 2. The basic parameters of DR.

Period Type	Period/h	$P_1(t)$ /[yuan·(kW·h)$^{-1}$]	$P_2(t)$ /[yuan·(kW·h)$^{-1}$]	$\rho(t)$
Peak Hours	[10, 15] and [20, 23]	1.00	1.25	0.8
Valley Period	[0, 8]	0.30	0.40	1.0
Normal Period	else	0.55	0.80	0.9

Table 3. The basic parameters of ESS.

Energy Storage Parameters	ESS1	ESS2	ESS3	ESS4
V_0/(MW·h)	20	30	15	25
$soc_{min,i}$	0.1	0.1	0.1	0.1
$soc_{max,i}$	0.9	0.9	0.9	0.9
$\eta_{ch,I}$, $\eta_{dis,i}$	0.8	0.8	0.8	0.8
$c_{ESS,i}$/[yuan·(kW·h^{-1})]	0.08	0.08	0.08	0.08

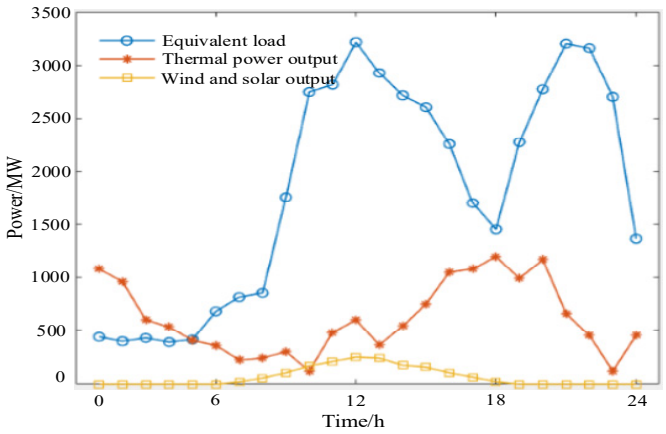

Figure 1. Load forecasting and theoretical output of wind power photovoltaic.

5.3. Scheduling Optimization Analysis

The hypothesis is to verify the effectiveness and practicability of the proposed model and to study the impact of DR and ESS on new energy absorption. The power generation dispatching of the system is divided into several scenarios for optimization analysis by MATLAB/Simulink 2023b simulation software.

Through the simulation experiment on scenarios 1–4, the corresponding equivalent load curve is shown in Figure 2, and the system optimization result is shown in Table 4. According to Figure 2, compared with the original load, the valley value of the equivalent load of the two-stage coordinated optimal scheduling during the valley period is higher

than that of the equivalent load with only the energy storage scheduling scheme. It reaches its peak at about 13:00. At this time, the peak value of the equivalent load of the two-stage coordinated optimal scheduling is even smaller than that of the equivalent load, with only the energy storage scheduling scheme and other peak periods having similar effects. This proves that the two-stage coordinated optimal scheduling improves load curves and has a better effect on peak-cutting and valley-filling.

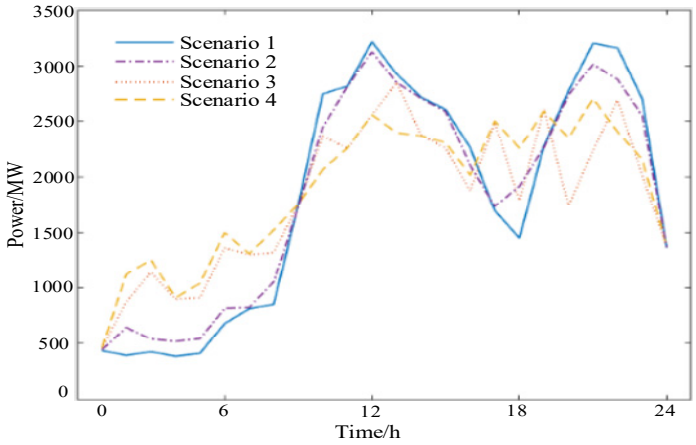

Figure 2. The curve of equivalent load.

Table 4. Optimization results under different scenarios.

Indicator	Scenario 1	Scenario 2	Scenario 3	Scenario 4
DR	No	No	Yes	Yes
ESS	No	Yes	No	Yes
S_{user}	1.00	1.00	0.74	0.76
μ	8.29	7.06	6.22	5.91
R_W	0.55	0.65	0.68	0.77
R_{PV}	0.97	0.96	0.98	0.99
R_{new}	0.63	0.68	0.70	0.81
C_1/10 thousand CNY	1174.25	1191.45	1192.11	1185.94
C_2/10 thousand CNY	0	58.23	59.76	65.12

According to Table 4, the proposed DR model effectively reduces the peak-to-valley ratio, which increases the absorption rate of new energy and ensures the smooth operation of the unit. After cooperating with ESS, the peak-to-valley ratio is further reduced, the level of new energy absorption is further improved, and the system is more stable. Combined with Figure 2, the reduction of the peak-to-valley ratio mainly improves the anti-peak regulation characteristics of wind energy, and the wind power absorption rate is significantly increased. The peak of photovoltaic output is consistent with the first peak of load, and the characteristic of anti-peak regulation is weak. After considering ESS, the discharge cost of ESS during the peak load period is much less than that of photovoltaic power generation. Affected by the lowest total cost of the system, the photovoltaic absorption rate may be slightly reduced, but the overall new energy absorption level still experiences a high degree of improvement.

As for the total operation cost, compared with scenario 1, the total cost of scenario 3 increased by CNY 178,600, and the total cost of scenario 4 increased by CNY 116,900; the new energy absorption level of scenarios 3 and 4 increased significantly, and the power generation cost was higher than that of thermal power, coupled with the call cost of ESS, so the total cost increased. The total cost of scenario 1 was low, but the peak and valley were relatively large, the system was not stable enough, and the safety and reliability were relatively low. For the problem of system adjustment cost, scenario 1 did not consider ESS and DR, so the value was 0; the adjustment cost of scenario 4 with comprehensive

consideration of DR and ESS increases by CNY 53,600 compared with scenario 3, but the total operating cost of the system was reduced by CNY 61,700, so the overall economy is better. At the same time, scenario 4 had the lowest peak-to-valley ratio and the highest new energy absorption rate. To sum up, the comprehensive effect of the proposed model, namely scenario 4, is optimal.

The comparison of equivalent load and unit output under Scenario 4 is shown in Figure 3. The DR load change is shown in Figure 4. From 16:00 to 19:00, the actual peak period of new energy output is also the peak period of electricity load. From 0:00 to 5:00, the peak period of new energy output no longer corresponds to the trough period of load, which also makes the output of thermal power units relatively stable and improves the safety and stability of the system.

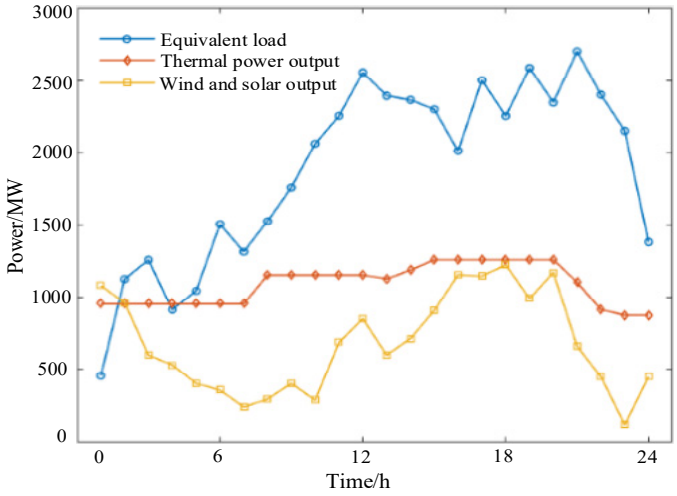

Figure 3. The comparison of equivalent load and unit output under scenario 4.

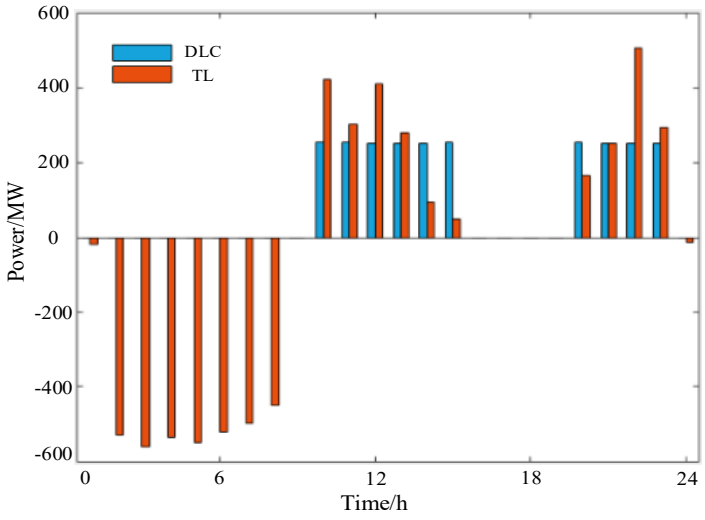

Figure 4. The demand response load changes under scenario 4.

From Figure 5a, when the load is at a low ebb, both the energy storage ESS1 and the energy storage ESS3 are in the charging state, and the charge of the energy storage ESS1 is less than that of the energy storage ESS3. According to Equation (20), during the whole valley period, the charge margin coefficient of energy storage ESS3 is larger than that of energy storage ESS1, so the scheduling priority of energy storage ESS3 is higher than that of energy storage ESS1. Therefore, when the system allocates power, the power allocated by the energy storage ESS3 is more than the energy storage ESS1.

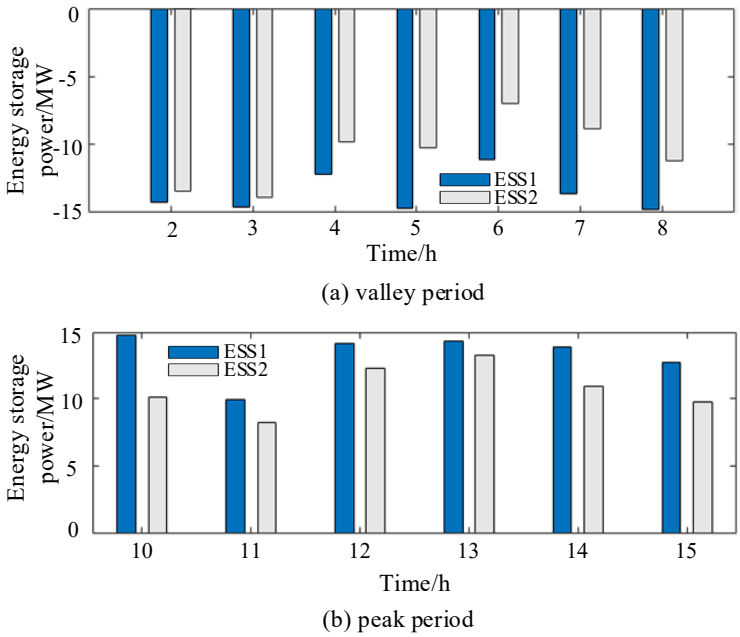

Figure 5. The comparison of energy storage output in different periods.

From Figure 5b, it can be seen that during the peak period of load, both energy storage ESS1 and energy storage ESS3 are in the state of discharge, and the discharge capacity of energy storage ESS1 is less than that of energy storage ESS3 during the peak period. During the whole valley period, the charging power of the energy storage ESS3 is greater than that of the energy storage ESS1, while in the peak period, the electricity of the energy storage ESS3 is larger than that of the energy storage ESS1. According to Equation (21), the discharge margin coefficient of energy storage ESS3 is larger than that of energy storage ESS1, so the scheduling priority of energy storage ESS3 is higher than that of energy storage ESS1. In general, the discharge of energy storage ESS3 is more than that of energy storage ESS1.

In order to reflect the superiority of the proposed DR model for different response groups over the conventional DR scheduling mode, generally only one response mode is considered. In this study, the new energy absorption rates of different proportions of DLC and TL project participation loads are compared, as shown in Figure 6. From Figure 6, the scheduling result considering different response modes is obviously better than that considering only one response mode, and the scheduling result is better with the increase of the proportion of the two response modes.

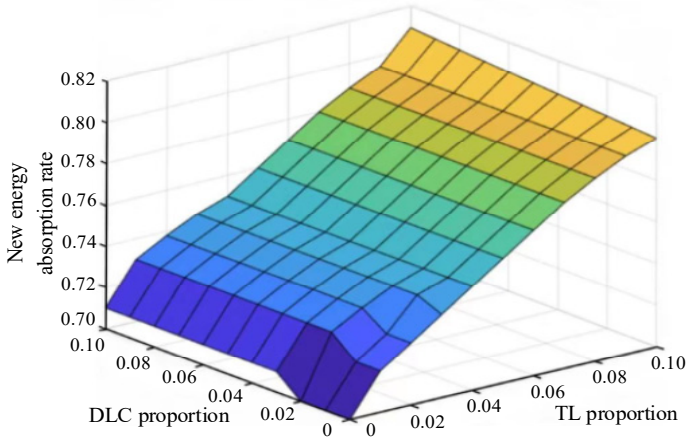

Figure 6. The new energy absorption rate under different demand response modes.

6. Conclusions

The reverse distribution of new energy output and load demand time is the main reason for a large number of abandonments of wind and light. In order to promote the large-scale grid connection of wind power and photovoltaic, a joint optimal scheduling model of wind and solar energy storage considering demand response is constructed based on the two-stage optimization theory. The results of numerical examples show the following:

1. The designed DR model effectively optimizes the demand-side load distribution. This, coupled with the call to the energy storage system, significantly improved the anti-peak regulation of new energy and increased the rate of new energy absorption.
2. The two-stage optimal scheduling model of landscape storage can optimize the output of the energy storage system (by modifying the day-ahead scheduling scheme), promote the energy storage system to participate in the optimal scheduling more reasonably, and improve the effect of peak-cutting and valley-filling.
3. The load peak-to-valley ratio is reduced through optimal dispatching; the output of the thermal power unit is more stable; the total cost is reduced; and the safety, reliability, and economic benefit of the system are improved.

The model proposed in this article has not yet taken into account the uncertainty and category of the load side, and the energy storage devices are relatively single. In subsequent research, the uncertainty of the load side and multiple types of energy storage devices can be added as research objects.

Author Contributions: Conceptualization, L.W.; Software, Y.L.; Validation, L.W.; Formal analysis, B.X. and K.X.; Resources, Y.L.; Writing—original draft, G.M.; Writing—review & editing, G.M.; Supervision, B.X. and K.X. All authors have read and agreed to the published version of the manuscript.

Funding: This research was funded by The Science and Technology Research Projects of Henan Provincial Department of Science and Technology, grant number 222103810093.

Data Availability Statement: The original contributions presented in the study are included in the article, further inquiries can be directed to the corresponding author.

Conflicts of Interest: The authors declare no conflict of interest.

References

1. Shu, Y.B.; Zhang, Z.G.; Guo, J.B.; Zhang, Z.L. Analysis of key factors of new energy absorption and research on solutions. *Proc. CSEE* **2017**, *37*, 1–8.
2. Tan, X.D.; Liu, J.; Xu, Z.C.; Yao, L.; Ji, G.Q.; Shan, B.G. Power supply and demand situation in the 14th five year plan under the "double carbon" goal. *Electr. Power* **2021**, *54*, 1–6.
3. Ju, L.W.; Yu, C.; Tan, Z.F. A two-stage scheduling optimization model and corresponding solving algorithm for power grid containing wind farm and energy storage system considering demand response. *Power Syst. Technol.* **2015**, *39*, 1287–1293.
4. Liu, W.Y.; Wen, J.; Xie, C.; Wang, W.Z.; Liang, C. Multi objective optimization method of power system source load coordination considering wind power absorption. *Proc. CSEE* **2015**, *35*, 1079–1088.
5. Stylianos, A.P. Integrated economic optimization of hybrid thermosolar concentrating system based on exact mathematical method. *Energies* **2022**, *15*, 7019.
6. Zang, H.; Ma, M.; Zhou, Y.; Xia, Q.; Sun, G.; Wei, Z. Robust optimal scheduling model for a 'wind power concentrating solar power-biomass' hybrid power plant in the electricity market. *Power Syst. Prot. Control* **2022**, *50*, 1–11.
7. Moretti, L.; Martelli, E.; Manzolini, G. An efficient robust optimization model for the unit commitment and dispatch of multi-energy systems and microgrids. *Appl. Energy* **2020**, *261*, 113859. [CrossRef]
8. Yu, D.; Sun, X.; Gao, B.T.; Xu, Q. Coordinated optimization model of wind power grid connection considering uncertain output of wind power. *Trans. China Electrotech. Soc.* **2016**, *31*, 34–41.
9. Mahmoud, N.; Saha, T.K.; Eghbal, M. Modelling demand response aggregator behavior in wind power offering strategies. *Appl. Energy* **2016**, *133*, 347–355. [CrossRef]
10. Mathieu, J.L.; Vayá, M.G.; Andersson, G. Uncertainty in the flexibility of aggregations of demand response resources. In Proceedings of the Industrial Electronics Society, IECON 2017, Vienna, Austria, 10–13 November 2017; pp. 8052–8057.
11. Zhou, J.; Yao, J.G.; Wang, K.; Shi, F.; Zeng, D. Continuous probabilistic power flow analysis method considering price type load response process. *Autom. Electr. Power Syst.* **2015**, *39*, 56–61.
12. Zhao, C.; Wang, J.; Watson, J.P.; Guan, Y. Multi-stage robust unit commitment considering wind and demand response uncertainties. *IEEE Trans. Power Syst.* **2012**, *280*, 2708–2717.

13. Niu, W.J.; Li, Y.; Wang, B.B. Modeling of demand response virtual power plant considering uncertainty. *Proc. CSEE* **2014**, *34*, 3630–3637.
14. Peng, C.H.; Liu, B.; Zuo, L.X.; Sun, H.J. Parallel multi-objective optimal scheduling of islanding microgrid considering classification demand response. *Power Syst. Prot. Control* **2019**, *47*, 60–68.
15. Li, P.; Xu, D.; Zhou, Z.; Lee, W.J.; Zhao, B. Stochastic optimal operation of microgrid based on chaotic binary particle swarm optimization. *IEEE Trans. Smart Grid* **2017**, *7*, 66–73. [CrossRef]
16. Liu, R.H.; Li, Z.L.; Yang, X.; Sun, G.P.; Li, L.H. The day ahead optimal scheduling of community integrated energy system considering user side flexible load. *Acta Energiae Solaris Sin.* **2019**, *40*, 2842–2850.
17. Qi, X.J.; Cheng, Q.; Wu, H.B.; Yang, S.H.; Li, Z.X. Influence of incentive demand response on distribution network operation reliability. *Trans. China Electrotech. Soc.* **2018**, *33*, 5319–5326.
18. Tang, W.; Gao, F. Recent optimal dispatching of household microgrid considering user satisfaction. *High Volt. Eng.* **2017**, *43*, 140–148.
19. Zhang, Z.Y.; Wang, W.L.; Zhang, G.; Wang, Z.W.; Ma, X.L.; Chu, Y.L. Evaluation method of new energy absorption capacity based on non time series model. *Autom. Electr. Power Syst.* **2019**, *43*, 24–30.